



**POLITECNICO**  
MILANO 1863

[RE.PUBLIC@POLIMI](mailto:RE.PUBLIC@POLIMI)

Research Publications at Politecnico di Milano

## Pre-Print

B. Arizmendi Gutierrez, A. Della Noce, M. Gallia, A.M.A. Guardone  
*Optimization of a Thermal Ice Protection System by Means of a Genetic Algorithm*  
in: *Bioinspired Optimization Methods and Their Applications*, B. Filipic, E. Minisci, M. Vasile  
(Eds.), Springer, 2020, ISBN: 9783030637095, p. 189-200[9th International Conference,  
BIOMA 2020, Brussels, Belgium, Nov. 19–20, 2020]  
doi:10.1007/978-3-030-63710-1\_15

The final publication is available at [https://doi.org/10.1007/978-3-030-63710-1\\_15](https://doi.org/10.1007/978-3-030-63710-1_15)

Access to the published version may require subscription.

**When citing this work, cite the original published paper.**

Permanent link to this version

<http://hdl.handle.net/11311/1154866>

# Optimization of a Thermal Ice Protection System by means of a Genetic Algorithm

Barbara Arizmendi Gutierrez, Alberto della Noce

Mariachiara Gallia, Alberto Guardone

Politecnico di Milano, Via Privata Giuseppe La Masa, 34, 20156 Milano MI, Italy  
barbara.arizmendi@polimi.it

**Abstract.** Ice accretion presents a major threat for performance and safety of aircraft. Electrothermal Ice Protection Systems present a reliable and flexible alternative to protect critical parts against it. Their main drawback is the high power consumption especially when operating in fully evaporative anti-ice mode. In this work, a genetic algorithm was deployed to optimize the power distribution on the fixed heaters of an electrothermal ice protection system for an airfoil operating in fully evaporative anti-ice mode. The GA is crossover based with a large population and no mutation. The reduction of the overall power consumption is sought. The objective function was constrained with the no-formation of ice in any location of the airfoil. The constraint has been included into the objective function by means of a penalty function. The freezing mass rate is numerically computed by means of the in-house developed code PoliMIce. The best solution encountered, could reduce the power consumption by 13.6% with respect to an intuitive design from literature. Moreover, the optimal layout of heat fluxes reduces the convective losses which are inefficiencies of the system.

**Keywords:** In-Flight Icing · Ice Protection System · Optimization · Genetic Algorithms

## Nomenclature

### Parameters

$\alpha$	Angle of attack [deg]	$MVD$	Mean Volume Diameter [ $\mu m$ ]
$\Delta l_i$	Size of the heater $i$ [ $m$ ]	$P_i$	Heat Flux of the heater $i$ [ $Wm^{-1}$ ]
$\Delta s_i$	Control volume surface area [ $m$ ]	$T$	Temperature [ $K$ ]
$\mathbf{P}$	Heat Fluxes vector	$v$	Velocity [ $ms^{-1}$ ]
$A$	Control volume surface area [ $m$ ]	<b>Subscripts</b>	
$c$	chord [ $m$ ]	0	Total
$c_p$	Specific heat [ $Jkg^{-1}K^{-1}$ ]	$\infty$	Free stream
$F$	Wetness fraction []	$ice$	Freezing
$H$	IPS Substratum thickness	$imp$	Impinging
$h$	Heat transfer coefficient [ $Wm^{-2}K^{-1}$ ]	$in$	Incoming to a control volume
$i_{l-s}$	Solidification latent heat [ $Jkg^{-1}$ ]	$out$	Outgoing from a control volume
$i_{l-v}$	Vaporization latent heat [ $Jkg^{-1}$ ]	$rec$	Recovery
$k_{wall}$	Effective solid conductivity	$ref$	Reference Temperature, 273.15K
$LWC$	Liquid Water Content [ $kgm^{-3}$ ]	$wall$	External solid surface
		$water$	Liquid film

## 1 Introduction

Ice accretion consists of the accumulation of ice on the surfaces of an aircraft when it interacts with supercooled clouds. These contain water droplets that are at a temperature below the freezing temperature but they remain liquid in a metastable equilibrium. When the droplets impact, they totally or partially freeze forming ice shapes [9]. Among other effects, it causes reductions in the lift capability, increase in drag, decrease of the control surface effectiveness [10]. Furthermore, severe ice accretions have been the cause of several accidents in the past [13]. According to literature, "the average altitude of icing environments is around 3000 m above mean sea level (msl), with few encounters above 6000 m" [14]. Commonly, aircraft surpass these altitudes during take-off and landing. For this reason, the critical parts of aircraft must be protected against ice, which include wings. There are two operational modes for IPS which are anti-ice and de-ice. Anti-Icing systems prevent the formation of ice whereas de-icing technologies remove an already formed layer of ice. Within the anti-ice mode, exists two sub-modes: fully evaporative and running wet. Electrothermal IPS is a mature technology, which has been widely deployed in small critical parts such as probes due to their reliability. It consists of a substratum including resistors to transform electricity into heating power [20]. One of its main drawbacks is its high power consumption compared to other technologies, specially in fully evaporative operation in large areas. Wing electrothermal IPS are deployed in several substratum bands that extend spanwise. In each band, a different thermal power can be allocated. Anti-ice operation requires a large amount of power supply sustained over the encounter of icing conditions. Despite its drawbacks, there is room for improvement and motivation for such in the development of fully electric aircraft.

There is a very limited research effort available in open literature concerning the experimental study of wing electrothermal IPS. This is due to the high costs and confidentiality. It is highlighted the work conducted by Al-Khalil[1], which consists of a set of icing wind tunnel tests of an electrothermal IPS. Due to the cost of experiments, there is a large research effort on the development of numerical models for the prediction of the performance of thermal anti-ice IPS. It

aims to support the preliminary design of these systems and to improve the understanding of the physics of the phenomenon. These codes include Antice[1], FENASP-ICE[2], and the works by Silva[18, 19] and Bu[4]. These models are based on the formulation of mass and energy conservation equations in a discrete surface. With the development of numerical codes, there is a recent research effort on optimizing the power consumption of thermal IPS. Pellisier [12] performed a surrogate-based numerical optimization of the geometric parameters of a thermal IPS in fully evaporative regime. The goal was to minimize the power consumption while ensuring all water was evaporated. Genetic Algorithms were selected for this purpose. The population size was 30 ran for 50 generations. Pourbagian performed a 2D surrogate-based optimization study of an electrothermal IPS for aircraft in both anti-ice and running wet operation modes[15]. The optimization algorithm selected was the gradient free Multi-Adaptive Direct Search (MADS). Further work of Pourbagian[16] included several formulations of objective functions and constraints for the Optimization of an electrothermal IPS.

In this work it is presented the numerical optimization of an electrothermal IPS working in fully evaporative mode. The numerical framework of optimization of the IPS includes only in-house developed or free-source codes. The optimization algorithm selected was a crossover based Genetic Algorithm. Particular focus is set on the understanding of the physics of optimal configurations compared with intuitive designs. The main goal is the understating of the link between the physics and an optimal performance. In the section 2, the framework for numerical simulations is presented. Section 3 describes the optimization methodology including the objective function selected. In section number 4, the results obtained will be presented and discussed. Finally in section 5 the concluding remarks are explained.

## 2 Numerical Modelling

### 2.1 Model Equations

The full numerical modelling of the complete physics of an electrothermal IPS is complex and it can be computationally demanding. In this work, several assumptions and simplifications have been

undertaken. Steady-state is assumed, given that generally, Ani-Ice systems deal with long exposures to icing conditions. The physics has been decomposed in several numerical steps that have been loosely coupled. A schematic view of the process is presented in the figure 1.

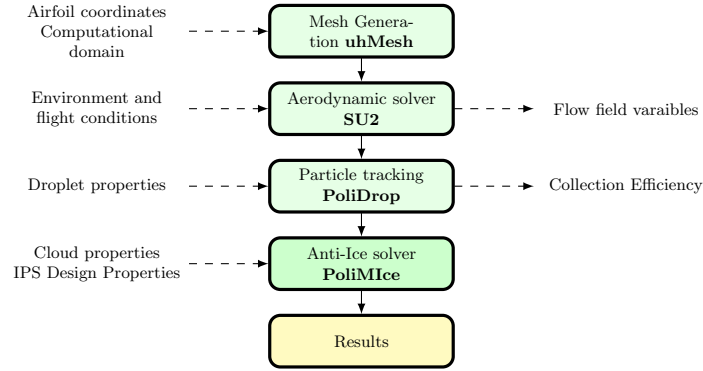


**Fig. 1.** Flow diagram of the numerical steps required for the modelling of anti-ice IPS. On the right hand side of the nodes the input values are presented whereas on the left hand side, the model outputs are shown

The initial step consists of the computation of the aerodynamic flow field which has been performed with the CFD code SU2[8]. The flow has been modelled as inviscid. The distribution of water impingement is computed by means of the in-house developed software PoliDrop [3]. Consists of a Lagrangian particle tracking solver which computes the trajectories of water droplets in an aerodynamic field. The thermal calculations are performed by the Anti-ice module of PoliMIce. The model equations are based in the work of da Silva[18, 17]. PoliMIce solves mass and energy conservation equations. These equations are solved in a discrete domain in control volumes. The mass conservation equation reads:

$$\dot{m}_{in} + \dot{m}_{imp} = \dot{m}_{out} + \dot{m}_{evap} + \dot{m}_{ice}. \quad (1)$$

The equation of the energy conservation in the solid substratum of the IPS is presented next:

$$\frac{d}{ds} \left( k_{wall} H \frac{dT_{wall}}{ds} \right) - F h_{water} (T_{wall} - T_{water}) + \dot{q}_{IPS}'' - (1 - F) [h_{air} (T_{wall} - T_{rec})] = 0 \quad (2)$$

Finally, a second conservation equation is formulated:

$$\begin{aligned}
& F A h_{air} (T_{rec} - T_{water}) + F A h_{water} (T_{wall} - T_{water}) \\
& + \dot{m}_{in} c_{p_{water}} (T_{in} - T_{ref}) - \dot{m}_{out} c_{p_{water}} (T_{out} - T_{ref}) \\
& + \dot{m}_{imp} \left[ c_{p_{water}} (T_{\infty} - T_{ref}) + \frac{V_{\infty}^2}{2} \right] - \dot{m}_e [i_{l-v} + c_{p_{water}} (T_{water} - T_{ref})] \\
& + \dot{m}_{ice} [i_{l-s} - c_{p_{water}} (T_{water} - T_{ref})] = 0.
\end{aligned} \tag{3}$$

The main heat fluxes in the film energy balance correspond to the evaporative and convective fluxes. The convective heat fluxes represent inefficiencies as ideally all the power would be devoted to evaporation. The evaporative heat flux depends exponentially on the temperature whereas the convective heat flux is linear. It is assumed there is no conduction across the height of the film. An icing term has been included to the conservation equations reported in [18]. In this case, the multiple layers of an IPS have been modelled as a unique layer with an equivalent thermal conductivity and a fixed thickness following the work of Silva[18]. The results obtained with

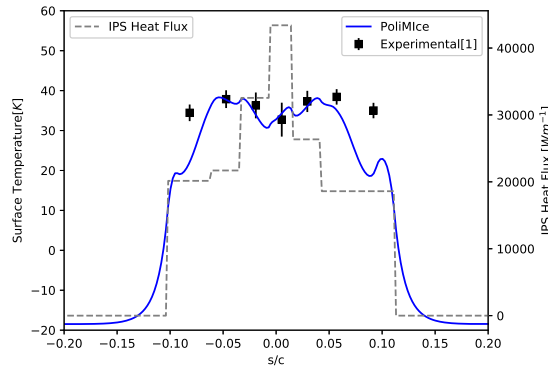


**Fig. 2.** Comparison of the experimental measurements of the surface temperature presented in Al-Khalil[1] and the predictions of the numerical model used in this work

the implementation of this model for the testcase 67 from the work of Al-Khalil[1] are presented in the figure 2. One can see that the computational results are in good agreement with the experimental results, in particular in the region of impingement.

## 2.2 Baseline Design

The layout of the IPS was taken from the experimental work of Al-Khalil[1]. The geometry consists of an extruded NACA0012 profile with a chord of 0.9144m. The IPS consists of a set of 7 symmetric multilayered heaters fitted at the leading edge. Due to a manufacturing issue, the heaters have been shifted towards the suction side a total of 0.0145m.

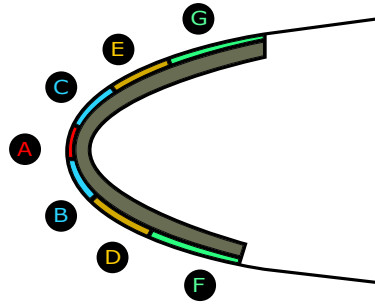


**Fig. 3.** Layout of the heaters of the electrothermal IPS. Note that due to a manufacturing issue the heaters are shifted towards the CEG side

Variable	Value
$T_0 [K]$	255.37
$v_\infty [ms^{-1}]$	89.41
$\alpha [^\circ]$	0
$LWC [gm^{-3}]$	0.55
$MVD [\mu m]$	20

**Table 1.** Flight and cloud properties for the test case 67A

Therefore, the geometry of the case is not symmetric and it is presented in the figure 3. This layout has been selected as the reference test-case for the optimization problem because it presents a realistic design with reasonable parameters. Moreover, the experimental test-case 67A has been selected as the baseline design to be compared with the optimal layout. The values of the cloud and flight properties are presented in the table . Due to the constant cloud and flight properties , the water impingement does not vary. Therefore, for the optimization of the heat fluxes, the solution of the aerodynamic field and the water impingement it only computed once. This will reduce the computational cost of sampling to the order of 20 seconds per sample.

### 3 Optimization Methodology

#### 3.1 Problem Formulation

The main drawback of large power consumption in electrothermal IPS motivates the study of design optimization. The end goal is the minimization this heating power while ensuring that no ice will be formed. The design vector  $\mathbf{P}$  includes the heat fluxes corresponding to each one of the 7 heaters. The no-formation of ice is included as a model constraint, considering that all the designs for which there is mass rate of water freezing greater than  $10^{-7}kg s^{-1}$  are unfeasible. Hence, the formulation of the optimization problem for a discrete domain reads:

$$\begin{aligned} & \text{minimize} && \sum_{i=1}^7 P_i \Delta l_i && (4a) \\ & \mathbf{P} \in \mathbb{R}^7 && && \end{aligned}$$

$$\text{subject to} \quad \sum_{i=1}^N \dot{m}_{ice}(s_i) = 0, \quad (4b)$$

$$P_i \geq 0m^{-2}, \quad (4c)$$

$$P_i \leq 45000m^{-2} \quad (4d)$$

**Constraint Handling** To deal with constraint, the penalty method was chosen[5]. It integrates the constraints into the objective function as a penalty. The penalty is proportional to the amount of constraint violation. In this case, it is proportional to the amount of extra-power that would be required to evaporate the mass rate of freezing water. The final formulation for the optimization problem is:

$$\begin{aligned} & \text{minimize} && \sum_{i=1}^7 P_i \Delta l_i - k \sum_{i=1}^N \dot{m}_{ice}(s_i) l_{l-v} && (5a) \\ & \mathbf{P} \in \mathbb{R}^7 && && \end{aligned}$$

$$\text{subject to} \quad P_i \geq 0Wm^{-2}, \quad (5b)$$

$$P_i \leq 45000Wm^{-2} \quad (5c)$$

Where k is an integer proportionality factor. Depending on the value set, low values will drive the optimization algorithm to the unfeasible region of the design space. High values will stop the optimization algorithm to explore the portions of the design space that are close to

the constraint. When the constraint is inactive, the objective function depends linearly on the heat fluxes and it can be computed from equation 5a. Further decrease of the heat fluxes will lead to the formation of ice in unprotected parts and the constraint will become active. At that point the monotony of the objective function will change due to the penalty. Then, it is expected that the global minima is found at the feasibility boundary.

### 3.2 Optimization Procedure

The objective function exhibits non-linear behaviour in the unfeasible region. The bounds of the feasible region are unknown a priori and it is possible that there are several local minima. In addition, the computational cost of sampling is short. For the reasons, stochastic and population based optimization algorithms are suitable [5]. Their drawbacks include large sampling required and slow convergence to the minima which in occasions is not reached. The nature-inspired genetic algorithm was chosen because it has been widely implemented and proven to be effective when appropriate parameters are set. Genetic Algorithms(GA) are inspired in the principle of evolution and the survival of the fittest with simple chromosome-like data encoding. A set of transformations are deployed into a population of designs. The survival is biased towards the most fit individuals, namely, the designs with minimal value of the objective function[11]. The number of bits selected for the binary coding dictates the desired accuracy of the design variables. In this case, 23 bits were required to attain an accuracy of 0.01, needing a total of 151 bits. The selected genetic operators for evolution and transformations are selection, crossover and elitism. In this case, a roulette wheel selection algorithm was chosen[11]. In a thorough study of the interactions between parameters, Deb [7] suggested crossover based GA are more reliable for an arbitrary problem. One point crossover between two individuals was selected with a probability of 0.9. Elitism operator was chosen to avoid losing optimal individuals due to randomness. Deb [7] also encouraged the selection of an appropriate population size, in this case a population of 500 individuals was chosen. This value is in the range of population values presented in Deb's work. To converge to a global minimum it is necessary to set an appropriate balance between exploration exploitation [6]. The exploration is attained by having a large and space filling initial population by

means of a latin hypercube design of experiments. The exploitation is performed by means of the selection and crossover operators. The convergence criteria was the computational time available, limiting it to 72 h.

## 4 Results

The value of the penalty factor  $k$  was set to 10 and the best solution found by the algorithm presented a power consumption of  $4174.63Wm^{-1}$ . The baseline design presented a performance of  $4815.82Wm^{-1}$ . That represents a reduction of 13.3% in power consumption. For lower values of  $k$  such as  $k=3$  the best solution found presented a performance of  $4064.81Wm^{-1}$ , however the constraint was violated as the ice mass rate was equal to  $2.53e-05 kgs^{-1}$ . The convergence history of the genetic algorithm is presented in the figure [?]. A to-

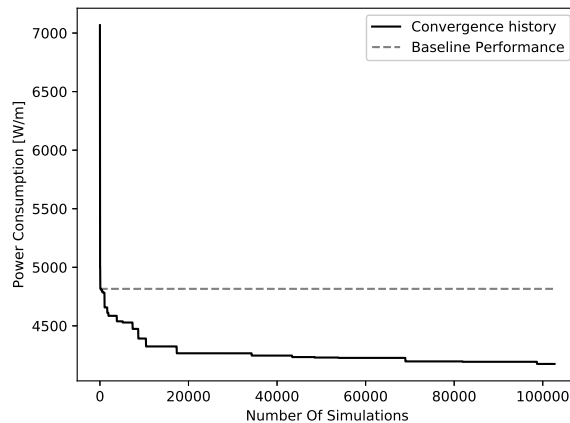


**Fig. 4.** Convergence history over the course of the simulations run in the available runtime. A much better performing solution has been found. However, the convergence on the objective function was not reached yet

tal of 102665 simulations were run over the computational budget. Despite the algorithm did not reach convergence, a better performing design from the baseline was found after 20000 simulations. The slow convergence could be due to the large bit representation of each individual, or to a suboptimal selection of GA parameters and operators.

Next, the comparison of the heat fluxes set for each heater is presented in table 2. For both designs, the water is fully evaporated within the protected part, before the heaters end limits. The maximum heat fluxes of the best design are located in heaters A, B and C. In this regions the maximum water impingement takes place, being the highest in heater A. In the case of the optimal design, the total power supplied by heaters A,B and C is larger. This leads to a more rapid evaporation, hence the liquid film will be shorter. Then, the water reaching heaters F and G will be limited, the thermal power requirements are reduced. Additionally, these heaters are the longest and therefore high heat fluxes there would lead to a drop in performance. Moreover, as part of the heater is dry, it is undesirable to set large heat fluxes there, as all the spare heat will be dissipated by the air stream.

Power [W/m]	Heater A	Heater B	Heater C	Heater D	Heater E	Heater F	Heater G
Baseline	43400	32550	26350	21700	18600	20150	18600
Optimal	36424.9	42929.5	42451.9	30090.8	17041.9	8.9	2887.6

**Table 2.** Comparison of the thermal heat fluxes of the baseline and optimal distributions of heat fluxes

Then, the surface temperature on the airfoil is presented in figure 5. One can see that for the optimal profile, the temperature is lower nearly in every location, reducing the convective losses in these locations. In two surface areas the temperature is higher. This correspond to the locations of the heaters B and C. The temperature raise exploits the dependence of the heat fluxes on temperature. That is, the exponential increase of the evaporative flux with temperature with respect to the linear increase of the convective flux. When a large power supplied in a heater, the energy heat fluxes going out of those control elements present a larger percentage devoted to evaporation than to convection, which is prominent at large temperatures. For this reason, more rapid evaporation occurs there and this reduces the thermal requirements downstream. The percentage of the supplied power transformed into convective losses is 33.8% whereas for the optimal it accounts for 30.5%. The optimality then resides in the reduction of the convective losses.

Additionally, the water temperature at the end of the film is identified in the figure 5 with black dashed lines. For both designs, the

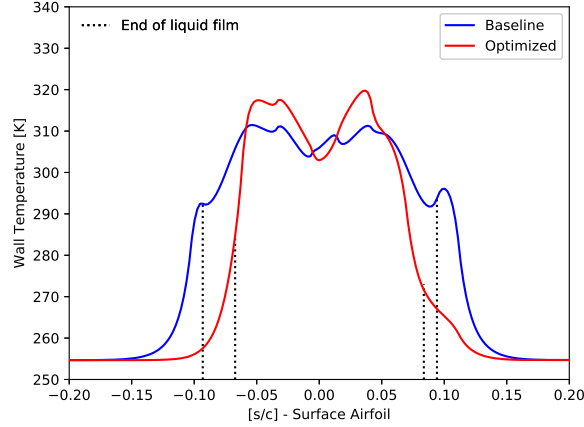


**Fig. 5.** Temperature predictions on the solid surface of the protected airfoil for baseline and optimal designs

water is fully evaporated within the protected part, before the heater limits. Ideally, the temperature at the end of the film should be close to the freezing temperature, such as it occurs in the suction side represented on the right of the figure ( $s/c \approx 0$ ). In that case, the reduction of any of the heat fluxes on that side of the airfoil would lead to ice formation and constraint violation. When this occurs in both sides of the airfoil, it represents a local minimum of the objective function. In this case, the temperature at the end of the liquid film in the pressure side ( $s/c \approx 0$ ) is equal to 290 K. Consequently, the heat supplied could be further reduced until the boundary of feasibility. For this reason, the solution found cannot be the global optimum solution or either a local minima, which is one of the drawbacks of Genetic Algorithms. Therefore, further investigation of the algorithm parameters would be required.

## 5 Final Remarks

The genetic algorithm successfully improved the initial intuitive design in terms of the performance metrics selected. That is, minimum power consumption constrained to the no-formation of ice. The best solution found is not the global optimum, because the power could be reduced extending the film on the pressure side. The computational cost was large requiring large number of samples, which is a

drawback of genetic algorithms. In order to find the global optimum, and to speed up the convergence, the parameters of the genetic algorithm must be investigated. Moreover, the binary encoding should be investigated as well. The accuracy set for the input (0.01) increased the poll of possible input combinations to  $2^{154}$ . This could have slowed down the convergence of the algorithm and the chances to find the global optimum.

It is concluded that an optimal design presents minimal overall convective losses for the same amount of evaporative fluxes. This can be achieved by increasing the water temperature in locations where there is a large water mass flux. Additionally, reducing the extension of the liquid film can help reduce the convective losses. Furthermore, the heat fluxes in dry parts should be low or otherwise, the convective losses will increase.

Due to the accuracy of the numerical model presented in section 2, it is expected a mismatch between the best solution here presented and reality. However, the qualitative design guidance here presented is expected to help on the allocation of heat fluxes on an electrothermal IPS.

**Acknowledgements.** The work in this paper was supported by the H2020-MSCAITN-2016 UTOPIAE, grant agreement 722734.

## References

1. Al-Khalil, K.M., Horvath, C., Miller, D.R., Wright, W.B.: Validation of nasa thermal ice protection computer codes. part 3; the validation of antice (2001)
2. Beaugendre, H., Morency, F., Habashi, W.G.: Fensap-ice's three-dimensional in-flight ice accretion module: Ice3d. *Journal of Aircraft* **40**(2), 239–247 (2003)
3. Bellosta, T.: A Lagrangian 3D particle tracking solver for in-flight ice accretion. Master's thesis, Politecnico di Milano (2019)
4. Bu, X., Lin, G., Yu, J., Yang, S., Song, X.: Numerical simulation of an airfoil electrothermal anti-icing system. *Proceedings of the Institution of Mechanical Engineers, Part G: Journal of Aerospace Engineering* **227**(10), 1608–1622 (2013)
5. Cavazzuti, M.: *Optimization methods: from theory to design scientific and technological aspects in mechanics*. Springer Science & Business Media (2012)
6. De Jong, K.: *Evolutionary computation: a unified approach* (2016)
7. Deb, K., Agrawal, S.: Understanding interactions among genetic algorithm parameters. pp. 265–286 (1998)
8. Economon, T.D., Palacios, F., Copeland, S.R., Lukaczyk, T.W., Alonso, J.J.: Su2: An open-source suite for multiphysics simulation and design. *Aiaa Journal* **54**(3), 828–846 (2016)
9. Gent, R., Dart, N., Cansdale, J.: Aircraft icing. *Philosophical Transactions of the Royal Society of London. Series A: Mathematical, Physical and Engineering Sciences* **358**(1776), 2873–2911 (2000)
10. Lynch, F.T., Khodadoust, A.: Effects of ice accretions on aircraft aerodynamics. *Progress in Aerospace Sciences* **37**(8), 669–767 (2001)

11. Michalewicz, Z.: Genetic algorithms+ data structures= evolution programs. Springer Science & Business Media (2013)
12. Pellissier, M., Habashi, W., Pueyo, A.: Optimization via fensap-ice of aircraft hot-air anti-icing systems. *Journal of Aircraft* **48**(1), 265–276 (2011)
13. Petty, K.R., Floyd, C.D.: A statistical review of aviation airframe icing accidents in the us. In: *Proceedings of the 11th Conference on Aviation, Range, and Aerospace Hyannis* (2004)
14. Politovich, M.: Aircraft icing. *Encyclopedia of Atmospheric Sciences* **358**(1776), 68–75 (2003)
15. Pourbagian, M., Habashi, W.G.: Surrogate-based optimization of electrothermal wing anti-icing systems. *Journal of aircraft* **50**(5), 1555–1563 (2013)
16. Pourbagian, M., Talgorn, B., Habashi, W.G., Kokkolaras, M., Le Digabel, S.: Constrained problem formulations for power optimization of aircraft electro-thermal anti-icing systems. *Optimization and Engineering* **16**(4), 663–693 (2015)
17. Silva, G., Silvaes, O., Zerbini, E., Hefazi, H., Chen, H.H., Kaups, K.: Differential boundary-layer analysis and runback water flow model applied to flow around airfoils with thermal anti-ice. In: *1st AIAA Atmospheric and Space Environments Conference*. p. 3967 (2009)
18. da Silva, G.A.L., de Mattos Silvaes, O., de Jesus Zerbini, E.J.G.: Numerical simulation of airfoil thermal anti-ice operation, part 1: mathematical modelling. *Journal of Aircraft* **44**(2), 627–633 (2007)
19. Silva, G.A.L.d., Silvaes, O.d.M., Zerbini, E.J.d.G.J.: Numerical simulation of airfoil thermal anti-ice operation, part 2: implementation and results. *Journal of aircraft* **44**(2), 634–641 (2007)
20. Wright, W., Keith, JR, T., De Witt, K.: Transient two-dimensional heat transfer through a composite body with application to deicing of aircraft components. In: *26th Aerospace Sciences Meeting*. p. 358 (1988)